

# Learning-based Robust and Secure Transmission for Reconfigurable Intelligent Surface Aided Millimeter Wave UAV Communications

Xufeng Guo, Ying Wang, *Member, IEEE*, and Yuanbin Chen

**Abstract**—In this letter, we study the secure transmission in the millimeter-wave (mmWave) unmanned aerial vehicle (UAV) communications assisted by the reconfigurable intelligent surface (RIS) under imperfect channel state information (CSI). Specifically, the active beamforming of the UAV, the coefficients of the RIS elements and the UAV trajectory are jointly designed to maximize the sum secrecy rate of all legitimate users in the presence of multiple eavesdroppers. However, the formulated problem is intractable mainly due to the complex constraints resulted from the intricate coupled variables and the time-related issue caused by outdated CSI. To tackle these difficulties, by leveraging the deep deterministic policy gradient (DDPG) framework, a novel and effective twin-DDPG deep reinforcement learning (TDDRL) algorithm is proposed. Simulation results demonstrate the effectiveness and robustness of the proposed algorithm, and the RIS can significantly improve the sum secrecy rate.

**Index Terms**—Deep reinforcement learning, reconfigurable intelligent surface, secure communication, UAV communication, millimeter-wave communications.

## I. INTRODUCTION

Millimeter-wave (mmWave) communications with multi-gigahertz bandwidth availability boost much higher capacity and transmission rate than conventional sub-6GHz communications. Unmanned aerial vehicles (UAVs), which are featured by their high mobility and flexible deployment, are promising candidates to compensate most of the deficiencies of mmWave signals, preserve its advantages, and provide more opportunities [1]. However, the mmWave signals transmitted by UAVs are prone to deteriorate due to their high sensitivity to the presence of spatial blockages, especially in the complex propagation environment (such as in urban areas), which thus degrades the reliability of the communication links. As a result, a more powerful and novel solution is more than essential.

Recently, the reconfigurable intelligent surface (RIS) composed of a large number of passive reflecting elements has become a revolutionary technology to achieve high spectral and energy efficiency in a cost-effective way [2]. By appropriately tuning the reflection coefficients, the reflected signal can be enhanced or weakened at different receivers. Since the RIS has significant passive beamforming gain, it can be

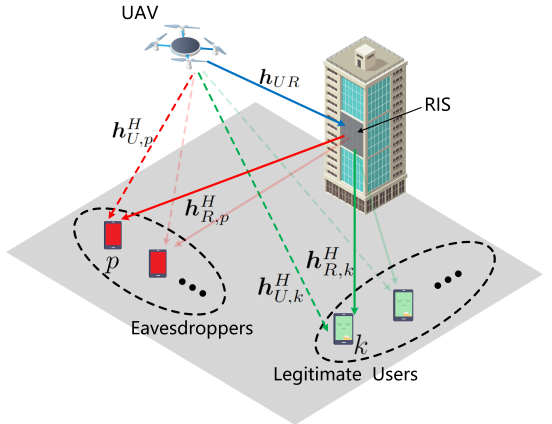


Fig. 1. RIS-aided Millimeter Wave UAV Communications.

incorporated into the mmWave UAV communication system to generate virtual LoS links, thereby achieving directional signal enhancement, expanding coverage area and reducing the need for radio frequency (RF) chains [3]. In addition, broadcasting and superposition, as two basic properties of the wireless communication, make wireless transmissions inherently susceptible to security breaches [4]. Hence, secure transmission is also a pivotal issue in UAV communication systems which attracted extensive interest of researches [5], [6].

A crucial issue in the RIS-aided mmWave UAV communication system is to jointly design the active and passive beamforming, and the UAV trajectory. However, unlike the general RIS-aided wireless communication model, the UAV mobility-induced variation of angles of arrival/departure (AoAs/AoDs) render the channel gains of all links (including direct links and cascaded links) to be optimization variables that need to be well-designed. Such variables are intricately coupled together with the active and passive beamforming matrix [7], which greatly increases the difficulty of the design. To circumvent this issue, several researches have been investigated in [5], [6], [8]–[10], some of which, in particular, leverage alternating optimization (AO) method [5], [6], [8], [9] to tackle the coupled variables, and adopt the phase alignment technique [8] for the single-user system. In [10], a deep reinforcement learning approach is utilized to jointly optimize the passive beamforming and the UAV trajectory, in which, however, the active beamforming is not considered in this approach. It should be pointed out that the above literature [5], [8]–[10] are based on the assumption of the perfect channel

Corresponding author: Ying Wang.

X. Guo, Y. Wang, and Y. Chen are with the State Key Laboratory of Networking and Switching Technology, Beijing University of Posts and Telecommunications, Beijing, China 100876 (e-mail:brook1711@bupt.edu.cn; wangying@bupt.edu.cn; chen\_yuanbin@163.com).

state information (CSI), which weakens the versatility and practicality of the model. Furthermore, the UAV mobility-induced outdated CSI should also be taken into account.

Due to good generalization, low complexity, and high accuracy, the deep reinforcement learning (DRL) is an efficient approach to jointly design the active and passive beamforming, and the UAV trajectory. The motivation of utilizing DRL approach is mainly for two reasons: i) it is fairly difficult to tackle the intricately couple variables in the RIS-aided system, and even the widely applicable AO method cannot solve this problem well, especially for the multi-user system. ii) the UAV mobility-induced CSI is easily outdated, and there is in general no effective method to solve such a time-related issue.

In this letter, motivated by these considerations, we investigate a secure transmission problem in an RIS-aided mmWave UAV communication system. The active beamforming at the UAV, the passive beamforming at the RIS, and the UAV trajectory are jointly designed by explicitly taking into account imperfect CSI. To enhance the robustness of the considered system, we study a secrecy rate maximization problem subject to the secrecy outage probability resulted from the statistical CSI error model. To solve this problem, a novel twin-deep deterministic policy gradient (TDDRL) deep reinforcement learning algorithm is proposed. More specifically, the first network is utilized to provide policy for the active and passive beamforming while the UAV trajectory is coordinated by the second network. The obtained simulation results demonstrate the effectiveness and the performance benefits of the proposed TDDRL algorithm.

## II. SYSTEM MODEL AND PROBLEM FORMULATION

### A. System Model

In this letter, we consider an RIS-aided mmWave UAV communication system where an RIS is exploited to assist the secure downlinks from the UAV to  $K$  single-antenna legitimate users in the presence of  $P$  single-antenna eavesdroppers. Specifically, the UAV is equipped with an  $A$ -element uniform linear array (ULA), and the RIS has a uniform planar array (UPA) with  $M=m^2$  passive reflecting elements ( $m$  should be an integer). The set of the legitimate users and the eavesdroppers are denoted by  $\mathcal{K}=\{1, 2, \dots, K\}$ ,  $\mathcal{P}=\{1, 2, \dots, P\}$ , respectively. As shown in Fig.1, all entities are placed in the three dimensional (3D) Cartesian coordinate system. The RIS is fixed at  $\mathbf{w}_R=(x_R, y_R, z_R)^T$ . We assume that the UAV flies at a fixed altitude in a finite time span which is divided into  $N$  time slots, i.e.,  $T=N\delta_t$ , where  $\delta_t$  is the time slot. Then the coordinate of the UAV and the coordinates of the legitimate users and eavesdroppers at the  $n$ -th time slot are denoted by  $\mathbf{q}[n]=(x_U[n], y_U[n], H_U)^T$ ,  $\mathbf{w}_i=(x_i[n], y_i[n], z_i[n])^T$ ,  $\forall i \in \mathcal{K} \cup \mathcal{P}$ , respectively. And the UAV subjects to the following mobility constraints:

$$\|\mathbf{q}[n+1] - \mathbf{q}[n]\|^2 \leq D^2, n = 1, \dots, N-1, \quad (1a)$$

$$|x[n]|, |y[n]| \leq B, n = 1, \dots, N, \quad (1b)$$

$$\mathbf{q}[0] \equiv (0, 0, H_U), n = 1, \dots, N-1. \quad (1c)$$

Let  $\mathbf{h}_{U,k} \in \mathbb{C}^{A \times 1}$ ,  $\mathbf{h}_{U,p} \in \mathbb{C}^{A \times 1}$ ,  $\mathbf{h}_{R,k} \in \mathbb{C}^{M \times 1}$ ,  $\mathbf{h}_{R,p} \in \mathbb{C}^{M \times 1}$ ,  $\mathbf{H}_{UR} \in \mathbb{C}^{M \times A}$  be the channel gains of the UAV to  $k$ -th user, the UAV to the  $p$ -th eavesdropper, the RIS to the  $k$ -th user, the RIS to the  $p$ -th eavesdropper, the UAV to the RIS links, respectively. All the channels are modeled according to 3D Saleh-Valenzuela channel model [11] [12] which has been widely used to characterize the mmWave channels:

$$\mathbf{h}_{U,i} = \sqrt{\frac{1}{L_{UK}}} \sum_{l=1}^{L_{UK}} g_{i,l}^u \mathbf{a}_L(\theta_{i,l}^{AoD}), \forall i \in \mathcal{K} \cup \mathcal{P}, \quad (2a)$$

$$\mathbf{h}_{R,i} = \sqrt{\frac{1}{L_{RK}}} \sum_{l=1}^{L_{RK}} g_{i,l}^r \mathbf{a}_P(\theta_{i,l}^{AoD}, \phi_{i,l}^{AoD}), \forall i \in \mathcal{K} \cup \mathcal{P}, \quad (2b)$$

$$\mathbf{h}_{UR} = \sqrt{\frac{1}{L_{RK}}} \sum_{l=1}^{L_{RK}} g_l^{ur} \mathbf{a}_P(\theta_l^{AoA}, \phi_l^{AoA}) \mathbf{a}_L(\theta_l^{AoD})^H. \quad (2c)$$

In (2), the large-scale fading coefficients defined by  $g \in \{g_{i,l}^u, g_{i,l}^r, g_l^{ur}\}$  follow a complex Gaussian distribution as  $\mathcal{CN}(0, 10^{\frac{PL}{10}})$ , where  $PL(\text{dB}) = -C_0 - 10\alpha \log_{10}(D) - PL_s$ ,  $C_0=61$  dB is the path loss at a reference distance of one meter,  $D$  (meters) is the link distance,  $\alpha$  denotes the path-loss exponent, and  $PL_s \sim \mathcal{CN}(0, \sigma_s^2)$  is the shadow fading component. The steering vector of the ULA is denoted by  $\mathbf{a}_L(\theta) = [1, e^{j\frac{2\pi}{\lambda_c}d \sin(\theta)}, \dots, e^{j\frac{2\pi}{\lambda_c}d(N-1) \sin(\theta)}]^H$  [13], where  $\theta$  stands for the azimuth angle of departure (AoD)  $\theta_{i,l}^{AoD}$  and  $\theta_l^{AoD}$ ,  $d$  is the antenna inter-spacing, and  $\lambda_c$  is the carrier wavelength. The steering vector of the UPA is denoted by  $\mathbf{a}_P(\theta, \phi) = [1, \dots, e^{j\frac{2\pi}{\lambda_c}d(p \sin(\theta) \sin(\phi) + q \cos(\theta) \sin(\phi))}, \dots]^H$  [13], where  $0 \leq p, q \leq m-1$ ,  $\theta(\phi)$  is the azimuth(elevation) AoD  $\theta_{i,l}^{AoD}(\phi_{i,l}^{AoD})$  and the angle of arrival (AoA)  $\theta_l^{AoA}(\phi_l^{AoA})$ .

The cascaded channel from the UAV to the  $i$ -th user or the eavesdropper can be written as  $\mathbf{H}_{C,i} = \text{diag}(\mathbf{h}_{R,i}^H) \mathbf{h}_{UR}$ ,  $\forall i \in \mathcal{K} \cup \mathcal{P}$ . The passive beamforming matrix [7] of the RIS is denoted by  $\Theta = \text{diag}(\beta_1 e^{j\theta_1}, \beta_2 e^{j\theta_2}, \dots, \beta_M e^{j\theta_M})$ , where  $\theta_m \in [0, 2\pi]$  and  $\beta_m \in [0, 1]$  represent the phase shift and amplitude reflection coefficient of the  $m$ -th RIS reflection element, respectively. The amplitude reflection coefficient subjects to unit-modulus constraints, i.e.,  $\beta_m=1$  to simplify the problem and maximize the power of the reflecting signal. Let  $\Psi = \text{vec}(\Theta)$  denote the vectorized passive beamforming vector. Thus, the received signal at the  $i$ -th user or eavesdropper from the UAV can be formulated as

$$y_i = (\mathbf{h}_{U,i}^H + \Psi^H \mathbf{H}_{C,i}) \mathbf{G} s + n_i, \forall i \in \mathcal{K} \cup \mathcal{P}, \quad (3)$$

where  $s_k$  with  $E[|s_k|^2]=1$  and  $\mathbf{G} \in \mathbb{C}^{A \times K}$  represents the transmitted symbol and the beamforming matrix at the UAV, and it is assumed that  $n_i \sim \mathcal{N}(0, \sigma_n)$ ,  $\forall i \in \mathcal{K} \cup \mathcal{P}$ . Let  $\mathbf{g}_k$  be the  $k$ -th column of the beamforming matrix  $\mathbf{G}$ . Then, the achievable unsecured rate of the  $k$ -th user is given by

$$R_k^u = \log_2 \left( 1 + \frac{|(\mathbf{h}_{U,k}^H + \Psi^H \mathbf{H}_{C,k}) \mathbf{g}_k|^2}{\sum_{k' \in \mathcal{K} \setminus \{k\}} |\mathbf{h}_{U,k'}^H + \Psi^H \mathbf{H}_{C,k'} \mathbf{g}_{k'}|^2 + n_k^2} \right). \quad (4)$$

If the  $p$ -th eavesdropper aims to eavesdrop the signal of the  $k$ -th user, its achievable rate can be denoted by

$$R_{p,k}^e = \log_2 \left( 1 + \frac{|(\mathbf{h}_{U,p}^H + \Psi^H \mathbf{H}_{C,p}) \mathbf{g}_k|^2}{\sum_{k' \in \mathcal{K} \setminus k} |\mathbf{h}_{U,p}^H + \Psi^H \mathbf{H}_{C,p}) \mathbf{g}_{k'}|^2 + n_p^2} \right). \quad (5)$$

The achievable individual secrecy rate from the UAV to the  $k$ -th user [14] can be expressed by

$$R_k^{\text{sec}} = \left[ R_k^{\text{u}} - \max_{\forall p} R_{p,k}^e \right]^+, \quad (6)$$

where  $[z]^+ = \max(0, z)$ .

It is worth noting that the outdated CSI will lead to substantial performance loss in practical systems. According to [15], the outdated CSI can be expressed as statistical CSI error model. Furthermore, let  $T_d$  be the delay between the outdated CSI and the real-time CSI. The relation between the outdated channel vector  $\mathbf{h}(t)$  and the real-time channel vector  $\mathbf{h}(t + T_d)$  can be expressed as [16]

$$\mathbf{h}(t + T_d) = \rho \mathbf{h}(t) + \sqrt{1 - \rho^2} \mathbf{e}, \quad (7)$$

where  $\mathbf{e}$  is independent identically distributed (i.i.d) with  $\mathbf{h}(t + T_d)$  and  $\mathbf{h}(t)$ ,  $\rho$  is the autocorrelation function of the channel gain  $\mathbf{h}(t)$ , given by the zeroth-order Bessel function of the first kind as  $\rho = J_0(2\pi f_D T_d)$ , where  $f_D$  is the Doppler spread which is expressed as  $f_D = v f_c / c$ , where  $v$ ,  $f_c$ ,  $c$  represent the velocity of the transceivers, the carrier frequency and the speed of light, respectively.

Then, the actual channel coefficients can be rewritten as

$$\begin{aligned} \mathbf{h}_{U,i} &= \rho \tilde{\mathbf{h}}_{U,i} + \Delta \mathbf{h}_{U,i}, \forall k \in \mathcal{K} \cup \mathcal{P}, \\ \mathbf{h}_{R,i} &= \rho \tilde{\mathbf{h}}_{R,i} + \Delta \mathbf{h}_{R,i}, \forall k \in \mathcal{K} \cup \mathcal{P}, \\ \mathbf{h}_{UR} &= \rho \tilde{\mathbf{h}}_{UR} + \Delta \mathbf{h}_{UR}. \end{aligned} \quad (8)$$

Note that the system only has access to the estimated CSI  $\tilde{\mathbf{h}} \in \{\tilde{\mathbf{h}}_{U,i}, \tilde{\mathbf{h}}_{R,i}, \tilde{\mathbf{h}}_{UR}\}$ , which are outdated, to generate active and passive beamforming and UAV trajectory. The actual CSI  $\mathbf{h} \in \{\mathbf{h}_{U,i}, \mathbf{h}_{R,i}, \mathbf{h}_{UR}\}$  is employed to calculate achievable secrecy rate of each user which has been expressed in (4), (5), (6).

### B. Problem Formulation

In this letter, we aim to maximize the sum secrecy rate  $\sum_{k=1}^K R_k^{\text{sec}}$  by jointly optimizing the UAV's trajectory  $\mathbf{Q} \triangleq \{\mathbf{q}[n], n \in \mathcal{N}\}$  and the active (passive) beamforming matrix  $\mathbf{G}(\Theta)$ . The problem is formulated as

$$\max_{\mathbf{Q}, \mathbf{G}, \Theta} \sum_{k \in \mathcal{K}} R_k^{\text{sec}} \quad (9a)$$

$$\text{s.t.} \quad (1), \quad (9b)$$

$$\Pr \left\{ R_k^{\text{sec}} \geq R_k^{\text{sec}, \text{th}} \right\} \geq 1 - \rho_k, \forall k \in \mathcal{K}, \quad (9c)$$

$$\text{Tr} (\mathbf{G} \mathbf{G}^H) \leq P_{\max}, \quad (9d)$$

$$\theta_m \in [0, 2\pi], \forall m \in \mathcal{M}, \quad (9e)$$

where the secrecy rate outage constraint in (9c) guarantees that the probability that each legitimate user can successfully

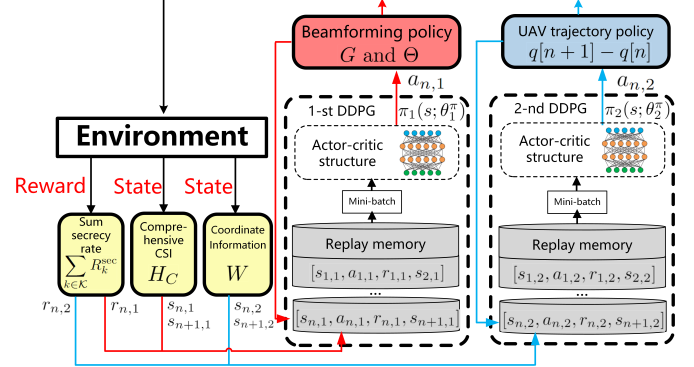


Fig. 2. Structure of the proposed TDDPG algorithm.

decode its message at a data rate of  $R_k^{\text{sec}, \text{th}}$  is no less than  $1 - \rho_k$ . Problem (10) is intractable mainly for the non-convex constraints in (10b), (10c), and (10e), the secrecy outage constraint without close-form, and the time varying CSI. There is in general no standard method to solve such a probability-constrained non-convex optimization. In Section III, a DRL-based approach is proposed to overcome these challenges effectively.

### III. DRL-BASED SOLUTION

To solve the non-convex problem in (9), we propose a TDDRL algorithm, instead of using single agent to find the optimal  $\mathbf{G}$ ,  $\Theta$  and  $\mathbf{Q}$ , since  $\mathbf{Q}$  would be highly coupled with large amounts of CSI using single agent which is actually irrelevant. As shown in Fig.2, the first network takes CSI as the state to obtain the optimal  $\mathbf{G}$  and  $\Theta$ , while the second network takes the coordinates of the UAV and all legitimate users and eavesdroppers as the state to obtain the UAV movement which consists of the flying distance  $\mu[n]$  and direction  $\psi[n]$  at the  $n$ -th time slot. Both networks take the sum secrecy data rate as reward. The overall algorithm for solving problem (9) is summarized in Algorithm 1.

The proposed TDDRL algorithm is based on DRL which is able to allow the agent to learn and build knowledge about the radio channels without knowing the channel models and mobility patterns [17]. Thus in the training mode the TDDRL algorithm is capable of optimizing policies while working in practical systems. In the working mode the training procedure can be cut out to reduce time cost, as the performance inclines to converge.

#### A. Active and Passive Beamforming

Inspired by the work of [14], the first DDPG-based network is employed to learn the optimal policy in terms of the UAV's beamforming matrix  $\mathbf{G}$  and the RIS's reflecting beamforming matrix  $\Theta$  by interacting with the whole system. Each episode is defined as a time span  $T$ , where each step is defined as a time slot  $\delta_n$ . In order to maximize the sum secrecy rate, the state  $s_{n,1}$ , the action  $a_{n,1}$ , the reward  $r_{n,1}$  in  $n$ -th time slot of the first agent is defined as follows:

- 1) **State**  $s_{n,1}$ : the state of the first agent in  $n$ -th time slot contains the estimated comprehensive CSI from the UAV

**Algorithm 1** TDDRL Algorithm

- 1: Initialize the actor and critic networks  $\pi_1(s; \theta_1^\pi)$ ,  $Q_1(s, a; \theta_1^Q)$ , target actor and critic networks  $\pi'_1(s; \theta_1^{\pi'})$ ,  $Q'_1(s, a; \theta_1^{Q'})$  of the first DDPG network;
- 2: Similarly, Initialize  $\pi_2(s; \theta_2^\pi)$ ,  $Q_2(s, a; \theta_2^Q)$ ,  $\pi'_2(s; \theta_2^{\pi'})$ ,  $Q'_2(s, a; \theta_2^{Q'})$  for the second DDPG network;
- 3: **for** Episode  $n_{ep} = 1, 2, \dots, N_{ep}$  of the second DDPG network **do**
- 4:   Reset the positions of the UAV and all users;
- 5:   **for** Step  $n = 1, 2, \dots, N_{step}$  **do**
- 6:     Observe  $\mathbf{H}_C$  as  $s_{n,1}$ , and  $\mathbf{W}$  as  $s_{n,2}$ ;
- 7:     Select actions  $a_{n,1}, a_{n,2}$  with a gaussian action noise  $n_a$  with variance  $\sigma_a$  :  

$$a_{n,1} = \pi_1(s; \theta_1^\pi) + n_a, a_{n,2} = \pi_2(s; \theta_2^\pi) + n_a$$
- 8:     Execute actions  $a_{n,1}, a_{n,2}$ , receive an immediate reward  $r_{n,1}$  According to Eq. (10) and receive new states  $s_{n+1,1}, s_{n+1,2}$  from the environment. Note that  $r_{n,1} = r_{n,2}$ ;
- 9:     Store the transitions  $[s_{n,1}, a_{n,1}, r_{n,1}, s_{n+1,1}]$  and  $[s_{n,2}, a_{n,2}, r_{n,2}, s_{n+1,2}]$  into the memory queues;
- 10:    Sample mini batchs to update  $\theta_i^\pi, \theta_i^Q, i \in \{1, 2\}$  [10];
- 11:    Update  $\theta_i^{\pi'}, \theta_i^{Q'}, i \in \{1, 2\}$ ;
- 12:   **end for**
- 13: **end for**

to all legitimate users and eavesdroppers, i.e.,  $\mathbf{H}_C \triangleq \{\mathbf{h}_{U,i}^H + \Psi^H \mathbf{H}_{C,i}\}, \forall i \in \mathcal{K} \cup \mathcal{P}$ .

- 2) **Action**  $a_{n,1}$ : we define the phase shift of all RIS reflecting elements  $\theta_m, \forall m \in \mathcal{M}$  and the transmit beamforming matrix  $\mathbf{G}$  as action. It is worth noting that  $\mathbf{G} = Re\{\mathbf{G}\} + Im\{\mathbf{G}\}$  and  $\Theta = Re\{\Theta\} + Im\{\Theta\}$  are separated as real part and imaginary part to tackle with the real input problem.
- 3) **Reward**  $r_{n,1}$ : the reward function is defined as:

$$r_{n,1} = \tanh\left(\sum_{k=1}^K R_k^{\sec} - p_r - p_m\right), \quad (10)$$

where  $p_r$  is the penalty if the outage constraint (9c) is not satisfied, and  $p_m$  is the the penalty when the UAV flies out of the target area. The value of the outage probabilities at each time step are estimated by 500  $\mathbf{H}_C$  samples generated according to the statistical CSI error model in (8). The hyperbolic tangent function  $\tanh(\cdot)$  is exploited to limite the reward in range of  $(-1, 1)$  for a better convergence.

### B. UAV Trajectory

The second DDPG network is exploited to simultaneously obtain the optimal movement  $\mu[n], \psi[n]$  with  $\mathbf{G}$  and  $\Theta$ . The state  $s_{n,2}$ , the action  $a_{n,2}$ , the reward  $r_{n,2}$  in  $n$ -th time slot of the second agent is defined as follows:

- 1) **State**  $s_{n,2}$ : as mentioned before, the UAV trajectory is rarely relevant to the large amounts of CSI. Thus, we take the coordinate information  $\mathbf{W} \triangleq \{\mathbf{q}[n]\} \cup \{\mathbf{w}_i[n] \forall i \in \mathcal{K} \cup \mathcal{P}\}$  as the state of the second network.

**TABLE I**  
MAIN PARAMETERS.

Parameter	Value
UAV antennas number	$A = 4$
RIS reflecting elements	$M = 16$
eavesdropper number	$P = 1$
legitimate user number	$K = 2$
step number	$N_{step} = 100$
episode number	$N_{ep} = 100$
carrier frequency	$f_c = 28 \text{ GHz}$
max transmission power	$P_{max} = 30 \text{ dBm}$
noise power	$\sigma_n = -114 \text{ dBmW}$
path loss factor [18]	$\alpha_{ur} = 2.2, \alpha_u = 3.5, \alpha_r = 2.8$
shadow fading factor	$\sigma_s = 3 \text{ dB}$

- 2) **Action**  $a_{n,2}$ : the action contains the UAV's flying distance  $\mu[n]$  and the direction  $\psi[n]$ . Then, the movement of UAV can be expressed as:

$$\mathbf{q}[n+1] - \mathbf{q}[n] = \mu[n](\cos\psi[n]\mathbf{e}_x + \sin\psi[n]\mathbf{e}_y) \quad (11)$$

- 3) **Reward**  $r_{n,2}$ : the same reward function in (10) is employed, since both network have the same objective to maximize the sum secrecy rate.

### C. Computational Complexity Analysis

This subsection mainly discusses the computational complexity of the proposed TDDRL algorithm. In particular, let  $L, n_i$  denote the layers number of the DNN exploited in the DDPG networks and the neurons number in the  $i$ -th layer, respectively. For the training mode, the computational complexity for a single DNN to both deliver actions and update in a single step is  $\mathcal{O}((N_b + 1)(\sum_{i=1}^{L-1} n_i n_{i+1}))$ , where  $N_b$  is the size of mini-batch. Since the TDDRL algorithm is composed of finite number of DNNs, and it takes  $N_{ep} * N_{step}$  steps to finish training, the training computational complexity of the TDDRL algorithm is  $\mathcal{O}(N_{ep} N_{step} (N_b + 1)(\sum_{i=1}^{L-1} n_i n_{i+1}))$ . For working mode, the computational complexity in each step dramatically decreases to  $\mathcal{O}(\sum_{i=1}^{L-1} n_i n_{i+1})$  due to the absence of the training procedure. So the time cost of the TDDRL algorithm significantly decreases as the traning procedure is finished.

## IV. SIMULATION RESULTS

In this section, numerical results are presented to evaluate the performance of our proposed TDDRL algorithm. For the first DDPG network, we deploy four fully-connected hidden layers with [800, 600, 512, 256] neurons in both actor and critic networks and the Adam optimizer is used to train the actor network with learning rate 0.0001 and critic network with learning rate 0.001. The second network has the same structure as the first network, but with different number of four layers [400, 300, 256, 128]. The initial coordinates of UAV and RIS are set as (0, 25, 50), (0, 50, 12.5). The eavesdropper is placed at (47, -4, 0). Furthermore, we model two legitimate users' movement as uniform motion in a straight line as shown in Fig.3. More detailed parameters are shown in Tabel I.

Fig.3 illustrates the optimized trajectory, which eventually converges as the learning procedure is over. It can be observed

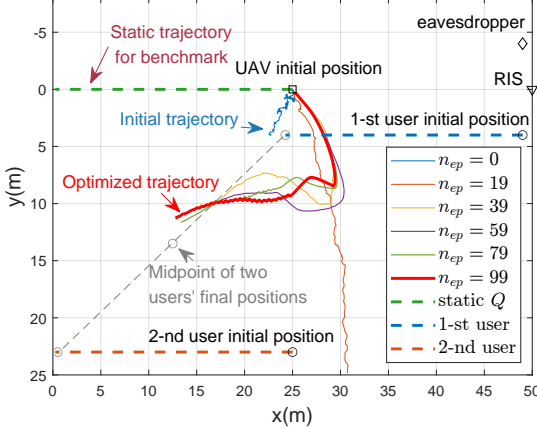


Fig. 3. Trajectory of the UAV optimized by the proposed TDDRL algorithm.

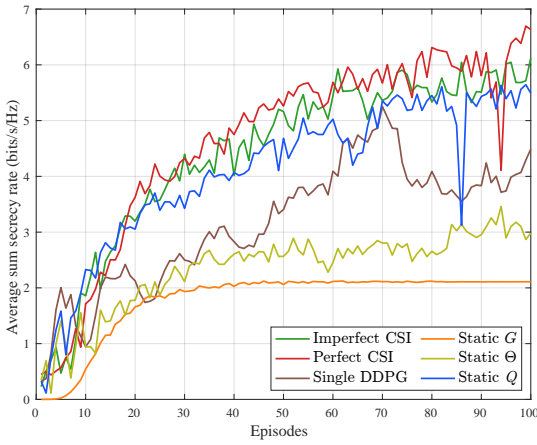


Fig. 4. Accumulated reward performance versus episodes under different RIS elements number.

that the UAV tends to move away from the eavesdropper. Moreover, the UAV is inclined to chase and follow the midpoint of two users position, while keeping relatively close distance to the RIS. This implies the UAV trajectory is jointly optimized with the active and passive beamforming, and the proposed algorithm can adapt to dynamic conditions brought by the users' mobility.

Fig. 4 plots the average sum secrecy rate versus, where the following benchmarks are used for comparison: 1) the propose **TDDRL algorithm under imperfect CSI**; 2) the proposed **TDDRL under perfect CSI**; 3) jointly design  $\mathbf{G}$ ,  $\boldsymbol{\Theta}$  and  $\mathbf{Q}$  with a single DDPG network; 4) jointly design  $\boldsymbol{\Theta}$  and  $\mathbf{Q}$  while using static  $\mathbf{G}$ ; 5) using static  $\boldsymbol{\Theta}$ ; 6) using static  $\mathbf{Q}$ . It is found that the proposed TDDRL algorithm which jointly optimizes  $\mathbf{G}$ ,  $\boldsymbol{\Theta}$  and  $\mathbf{Q}$  achieves the best performance under imperfect CSI. Compared with the single DDPG scheme, the proposed TDDRL algorithm has a better convergence and performance by configuring the same learning rate and layer number. However, the proposed TDDRL algorithm performs slightly better under the perfect CSI, which implies the proposed TDDRL has a good robustness. To sum up, the secrecy rates of legitimate users in our proposed system under imperfect CSI can be maximized leveraging RIS and UAV by the proposed TDDRL algorithm.

## V. CONCLUSION

In this letter, we investigate robust and secure transmission for RIS-aided mmWave UAV communications. To maximize the secrecy rates of legitimate users, we proposed a TDDRL algorithm to effectively tackle the concerned issues. Simulation results validated that by jointly optimizing UAV trajectory and active (passive) beamforming, a better performance can be achieved under imperfect CSI compared with other benchmarks.

## REFERENCES

- [1] C. Zhang, W. Zhang, W. Wang, L. Yang, and W. Zhang, "Research challenges and opportunities of UAV millimeter-wave communications," *IEEE Wireless Commun.*, vol. 26, no. 1, pp. 58–62, Feb. 2019.
- [2] M. Di Renzo, A. Zappone, M. Debbah, M. S. Alouini, C. Yuen, J. de Rosny, and S. Tretyakov, "Smart radio environments empowered by reconfigurable intelligent surfaces: How it works, state of research, and the road ahead," *IEEE J. Sel. Areas Commun.*, vol. 38, no. 11, pp. 2450–2525, Nov. 2020.
- [3] A. S. Abdalla, T. F. Rahman, and V. Marojevic, "UAVs with reconfigurable intelligent surfaces: Applications, challenges, and opportunities," Dec. 2020. [Online]. Available: <https://arxiv.org/pdf/2012.04775.pdf>
- [4] X. Yu, D. Xu, Y. Sun, D. W. K. Ng, and R. Schober, "Robust and secure wireless communications via intelligent reflecting surfaces," *IEEE J. Sel. Areas Commun.*, vol. 38, no. 11, pp. 2637–2652, Nov. 2020.
- [5] W. Wang, H. Tian, W. Ni, and M. Hua, "Intelligent reflecting surface aided secure UAV communications," Nov. 2020. [Online]. Available: <https://arxiv.org/pdf/2011.04339.pdf>
- [6] S. Li, B. Duo, M. Di Renzo, M. Tao, and X. Yuan, "Robust secure UAV communications with the aid of reconfigurable intelligent surfaces," Dec. 2020. [Online]. Available: <https://arxiv.org/pdf/2008.09404.pdf>
- [7] M. Zhao, Q. Wu, M. Zhao, and R. Zhang, "Two-timescale beamforming optimization for intelligent reflecting surface enhanced wireless network," in *Proc. IEEE SAM, Hangzhou, CN*, Jun. 2020.
- [8] S. Li, B. Duo, X. Yuan, Y. Liang, and M. Di Renzo, "Reconfigurable intelligent surface assisted UAV communication: Joint trajectory design and passive beamforming," *IEEE Wireless Commun. Lett.*, vol. 9, no. 5, pp. 716–720, May 2020.
- [9] M. Hua, L. Yang, Q. Wu, C. Pan, C. Li, and A. L. Swindlehurst, "UAV-assisted intelligent reflecting surface symbiotic radio system," Jan. 2021. [Online]. Available: <https://arxiv.org/pdf/2007.14029>
- [10] L. Wang, K. Wang, C. Pan, W. Xu, and N. Aslam, "Joint trajectory and passive beamforming design for intelligent reflecting surface-aided UAV communications: A deep reinforcement learning approach," Jul. 2020. [Online]. Available: <https://arxiv.org/pdf/2007.08380>
- [11] G. Zhou, C. Pan, H. Ren, K. Wang, M. Elkashlan, and M. D. Renzo, "Stochastic learning-based robust beamforming design for RIS-aided millimeter-wave systems in the presence of random blockages," *IEEE Trans. Veh. Technol.*, pp. 1–1, Jan. 2021.
- [12] Y. Cao, T. Lv, and W. Ni, "Intelligent reflecting surface aided multi-user mmwave communications for coverage enhancement," in *Proc. IEEE PIMRC, London, UK*, Aug. 2020.
- [13] S. K. Yong and J. S. Thompson, "A three-dimensional spatial fading correlation model for uniform rectangular arrays," *IEEE Antennas Wireless Propag. Lett.*, vol. 2, pp. 182–185, 2003.
- [14] H. Yang, Z. Xiong, J. Zhao, D. Niyato, L. Xiao, and Q. Wu, "Deep reinforcement learning-based intelligent reflecting surface for secure wireless communications," *IEEE Trans. Wireless Commun.*, vol. 20, no. 1, pp. 375–388, Jan. 2021.
- [15] G. Zhou, C. Pan, H. Ren, K. Wang, and A. Nallanathan, "A framework of robust transmission design for IRS-aided MISO communications with imperfect cascaded channels," *IEEE Trans. Signal Process.*, vol. 68, pp. 5092–5106, Aug. 2020.
- [16] Y. Huang, F. Al-Qahtani, C. Zhong, Q. Wu, J. Wang, and H. Alnuweiri, "Performance analysis of multiuser multiple antenna relaying networks with co-channel interference and feedback delay," *IEEE Trans. on Commun.*, vol. 62, no. 1, pp. 59–73, Jan. 2014.
- [17] C. Huang, R. Mo, and C. Yuen, "Reconfigurable intelligent surface assisted multiuser MISO systems exploiting deep reinforcement learning," *IEEE J. Sel. Areas Commun.*, vol. 38, no. 8, pp. 1839–1850, Aug. 2020.
- [18] X. Liu, Y. Liu, and Y. Chen, "Machine learning empowered trajectory and passive beamforming design in UAV-RIS wireless networks," *IEEE J. Sel. Areas Commun.*, pp. 1–1, Dec. 2020.